

## ON THE NUMERICAL MODELING FOR SURFACTANT FLOODING OF OIL RESERVOIRS

M. Susana Bidner\*<sup>†</sup> and Gabriela B. Savioli\*

\*Laboratorio de Ingeniería de Reservorios  
Facultad de Ingeniería, Universidad de Buenos Aires  
Ciudad Universitaria, Pabellón de Industrias, Universidad de Buenos Aires  
(1428) Buenos Aires, Argentina  
e-mail: sbidner@di.fcen.uba.ar, gsavioli@di.fcen.uba.ar

<sup>†</sup>Laboratorio de Reservorios  
Facultad de Ingeniería, Universidad Nacional de Cuyo  
Centro Universitario, Parque General San Martín, (5500) Mendoza, Argentina

**Key words:** numerical simulation, surfactant flooding, finite differences, two-phase three-component systems.

**Abstract.** *A surfactant flood model for a three-component (petroleum, water, surfactant), two-phase (aqueous, oleic) system is presented and analyzed. It is ruled by a system of non-linear, partial, differential equations: the continuity equation for the transport of each component, Darcy's equation for the flow of each phase and algebraic equations. This system is numerically solved in the one-dimensional case by finite differences using a procedure implicit in pressure and explicit in concentrations. The simulator is fed with the physical properties that are concentration dependent functions— such as phase behavior, interfacial tension, relative permeabilities, residual saturations, phase viscosities, adsorption and others. Measurement of these properties is difficult and sometimes hampered by couplings. That is why the main issue in simulation of surfactant flooding is the unavailability of data. Therefore, the purpose of this paper is twofold. First, to describe with detail those phase properties and their relationships. We have found that the partition of the three-components between the two-phases determines all other physical property data and hence the oil recovery. Second, to present a sensitivity analysis of the influence of that partition on cumulative oil recovered as a function of time.*

## 1 INTRODUCTION

Recovery from oil fields by natural drive mechanisms (e.g. solution gas drive, gas cap drive, water drive) is called Primary Recovery<sup>1</sup>. When oil production declines, gas or water are injected to maintain reservoir pressure. This process is called Secondary Recovery. Statistically, after a Secondary Recovery, more than half of the oil originally in place in the reservoir still remains trapped. The recovery of this trapped oil is the target of the Enhanced Oil Recovery processes. EOR implies the injection of materials not naturally present in the reservoir<sup>1,2</sup>. Among these materials, surfactants are injected to decrease the interfacial tension between oil and water in order to mobilize the oil trapped after secondary recovery by waterflooding.

In a surfactant flood a multicomponent, multiphase system is involved. The theory of multicomponent, multiphase flow has been presented by several authors<sup>3-6</sup> and applied to two-phase, three-component systems<sup>7-11</sup>. Those studies lead to the building of complex simulators, like the one developed at The University of Texas at Austin, UTCHEM, which has been first presented in the three companion papers of Camilleri *et al*<sup>12-14</sup> and most recently by Delshad *et al*<sup>15</sup>. UTCHEM with 19 components and 4 phases has incorporated most physical phenomena. For a Surfactant Pilot Simulation<sup>16</sup>, those physical phenomena were described in terms of more than 70 parameters.

A great deal of experimental research has been done to measure those parameters which represent physical property data for the numerical simulator<sup>12-16</sup>. Beyond the effort to measure these data, there is an additional problem: the parameters are highly complex and coupled. Because of that, it is difficult to analyze simultaneously occurring mechanisms. The aim of this paper is to contribute to this analysis.

We use a previously reported ternary two-phase model<sup>17,18</sup>, into which representative concentration-dependent physical properties have been added<sup>19,20</sup>.

The chemical flood model is represented by a system of nonlinear partial differential equations: the continuity equation for the transport of the components and Darcy's equation for the two-phase flow. It is solved by an iterative finite-difference procedure that allows implicit calculation of pressure and Darcy's velocities and explicit calculation of concentrations. The system of equations is completed with the equations representing physical properties of the fluids and the rock<sup>1</sup>.

Physical properties described here are: (1) phase behavior represented by a ternary diagram, (2) interfacial tension between both fluid phases, (3) residual phase saturations, (4) relative permeabilities, (5) rock wettability, (6) phase viscosities, (7) capillary pressure, (8) adsorption and (9) dispersion.

From a physical-chemical point of view, there are three components -water, petroleum and chemical. They are, in fact, pseudo-components, since each one consists of several pure components. Petroleum is a complex mixture of many hydrocarbons. Water is actually brine, and contains dissolved salts. Finally, the chemical may contain different kinds of surfactants, plus alcohols, polymers, etc.

These three pseudo-components are distributed between two phases -the oleic phase and

the aqueous phase. The chemical has an amphiphilic character. It makes the oleic phase at least partially miscible with water. Or the aqueous phase at least partially miscible with petroleum<sup>19</sup>.

Interfacial tension depends on the surfactant partition between the two phases, and hence of phase behavior<sup>9</sup>. Residual phase saturations decrease as interfacial tension decreases<sup>8</sup>. Relative permeability parameters depend on residual phase saturations<sup>9</sup>. Phase viscosities are functions of the volume fraction of the components in each fluid phase<sup>12</sup>.

Therefore, the success or failure of surfactant flooding processes depends on phase behavior. Phase behavior influences all other physical properties, and each of them, in turn, influences oil recovery.

## 2 MODEL DESCRIPTION

### 2.1 Assumptions

This model represents a laboratory displacement test. Initially the porous medium contains a residual saturation of oil that was left behind by a previous waterflood. Our assumptions are that the porous medium has a cross-sectional area  $A$ , porosity  $\phi$  and absolute permeability  $K$ ; all of which are constant. The flow is isothermal, one-dimensional and incompressible. There are an aqueous and an oleic phase and three components: water, petroleum and chemical. There is no volume change with the mixture of the components in each phase. The system is in local thermodynamic (phase) equilibrium. Darcy's law applies. Gravity forces are negligible compared with viscous forces.

### 2.2 Flow equations

Microscopic balances are applied to a representative elementary volume (REV) of the porous medium<sup>2,21</sup>. They are described by both Darcy's and continuity equations, defining momentum conservation for the flow of each phase and mass conservation for each component, respectively.

Considering the assumptions of the model, Darcy's phase velocities are

$$u^j = -K \frac{k_r^j}{\mu^j} \frac{\partial P^j}{\partial x}; \quad j = o, a \quad (1)$$

$k_r^j, \mu^j$  and  $P^j$  are the relative permeability, viscosity and pressure of phase  $j$ , respectively. The sum of both Equations 1 yields

$$u = -\lambda \frac{\partial P^a}{\partial x} - \lambda^o \frac{\partial P_C}{\partial x} \quad (2)$$

where  $P_C$  is the capillary pressure of the two-phase system defined as,

$$P_C = P^o - P^a \quad (3)$$

$\lambda$  and  $\lambda^j$  are, respectively, total and  $j$ -phase mobilities defined by,

$$\lambda = \lambda^o + \lambda^a \quad (4)$$

$$\lambda^j = \frac{Kk_r^j}{\mu^j}; \quad j = o, a \quad (5)$$

and  $u$  is total Darcy's velocity,

$$u = u^o + u^a \quad (6)$$

Continuity equations for the three components are,

$$\phi \frac{\partial Z_i}{\partial t} + \frac{\partial}{\partial x} \sum_j V_i^j u^j - \frac{\partial}{\partial x} \sum_j \phi S^j D_i^j \frac{\partial V_i^j}{\partial x} = -\frac{\partial Ad_i}{\partial t} \quad ; \quad i = p, c, w \quad (7)$$

$\phi$  is porosity;  $V_i^j$  and  $D_i^j$  are, respectively, the volume fraction and the dispersion coefficient of component  $i$  in phase  $j$ ;  $S^j$  is the saturation of phase  $j$ ;  $Ad_i$  is the adsorbed volume of component  $i$  per unit volume of the porous medium and  $Z_i$  is the overall volumetric concentration of component  $i$ , defined by

$$Z_i = \sum_j S^j V_i^j; \quad i = p, w, c \quad (8)$$

The following expressions provide the macroscopic volume balances,

$$\sum_i V_i^j = 1; \quad j = o, a \quad (9)$$

$$\sum_j S^j = 1 \quad (10)$$

$$\sum_i Z_i = 1 \quad (11)$$

The Equation for the aqueous phase pressure is obtained by combining the sum of Equations 7 over  $i$  with Equations 2, 6, 9 ( $j = o, a$ ), 10 and 11. Thus,

$$\frac{\partial}{\partial x} \left( \lambda \frac{\partial P^a}{\partial x} \right) = \frac{\partial}{\partial t} \left( \sum_i Ad_i \right) - \frac{\partial}{\partial x} \left( \lambda^o \frac{\partial P_c}{\partial x} \right) \quad (12)$$

So far, the model has 16 unknowns:  $u^j, u, P^j, S^j, V_i^j$  and  $Z_i$  ( $i = p, w, c; j = o, a$ ) but only 13 equations: Equations 1 ( $j = a$ ), 2, 3, 6, 7 ( $i = p, c$ ), 8 ( $i = p, c$ ), 9 ( $j = o, a$ ), 10 11 and 12. The phase relationships described in section 3.1 add three more equations (Eq. 22-24).

### 2.3 Initial and boundary conditions

Initially the reservoir contains oil at its waterflood residual oleic saturation,  $S^{orH}$ . There is no chemical component and the initial pressure is constant, therefore

$$t = 0 ; 0 \leq x \leq L : Z_c = 0 ; Z_p = S^{orH} ; P^a = P_i \quad (13)$$

At inlet an aqueous solution of a constant composition chemical slug is injected during a time  $t_s$  followed by a continuous bank of water. The flow rate and the chemical concentration are both constant, thus

$$x = 0 ; 0 < t \leq t_s : Z_c = Z_c^{IN} ; Z_p = Z_p^{IN} \quad (14)$$

$$t > t_s : Z_c = 0 ; Z_p = 0$$

$$x = 0 ; t > 0 : -\lambda \frac{\partial P^a}{\partial x} = u^{IN} \quad (15)$$

where superscript *IN* means injected value. At outlet, Neuman conditions for the overall concentrations are applied. Besides, pressure is constant. Therefore

$$x = L ; t > 0 : \frac{\partial Z_i}{\partial x} = 0, i = p, c ; P^a = P_e \quad (16)$$

### 2.4 Discretization of the differential equations

The differential Equations 1 ( $j = a$ ), 2, 7 ( $i = p, c$ ) and 12 are numerically solved by finite-differences, using an iterative procedure which takes into account the nonlinearities. The aqueous phase pressure, total Darcy's velocity and the aqueous phase velocity are implicitly solved using the following centered-difference equations for the discretization of Equations 12, 2 and 1 ( $j = a$ ), respectively,

$$\lambda_{m+1}^{n+1,k} (P_{m+1}^a - P_m^a)^{n+1,k+1} - \lambda_m^{n+1,k} (P_m^a - P_{m-1}^a)^{n+1,k+1} =$$

$$= \frac{\Delta x^2}{\Delta t} (Ad^{n+1,k} - Ad^n) - \left[ \lambda_{m+1}^o (P_{C_{m+1}} - P_{C_m}) - \lambda_m^o (P_{C_m} - P_{C_{m-1}}) \right]^{n+1,k} \quad (17)$$

$$(u)_m^{n+1,k+1} = -\lambda_m^{n+1,k} \left( \frac{P_{m+1}^a - P_{m-1}^a}{2\Delta x} \right)^{n+1,k+1} - (\lambda^o)_m^{n+1,k} \left( \frac{P_{C_{m+1}} - P_{C_{m-1}}}{2\Delta x} \right)^{n+1,k} \quad (18)$$

$$(u^a)_m^{n+1,k+1} = -(\lambda^a)_m^{n+1,k} \left( \frac{P_{m+1}^a - P_{m-1}^a}{2\Delta x} \right)^{n+1,k+1} ; \quad 2 \leq m \leq NX - 1 \quad (19)$$

$k$  is the iteration level,  $NX$  is the total number of grid-blocks,  $\Delta x$  and  $\Delta t$  are the space and time increments,  $m$  indicates the grid-block and  $n$  indicates the time-step. The treatment of non-linearities in Equations 17, 18 and 19 is the standard practice in reservoir simulation<sup>18,22</sup>.

The overall concentrations of Equations 7 ( $i = p, c$ ) are explicitly solved; the convective term is solved by backward differencing and the dispersive term by central differencing according to

$$\begin{aligned} & \frac{\phi}{\Delta t} (Z_i^{n+1} - Z_i^n)_m + \frac{1}{\Delta x} \sum_j (u_m^{j,n+1,k+1} V_{i,m}^{j,n+1,k} - u_{m-1}^{j,n+1,k+1} V_{i,m-1}^{j,n+1,k}) - \\ & - \frac{1}{\Delta x^2} \sum_j \left[ (S^j D_i^j)_{m+1/2} (V_{i,m+1}^j - V_{i,m}^j) - (S^j D_i^j)_{m-1/2} (V_{i,m}^j - V_{i,m-1}^j) \right]^{n+1,k} = \quad (20) \\ & = (Ad_i^n - Ad_i^{n+1})_m^k / \Delta t \quad ; \quad i = p, c \quad ; \quad 2 \leq m \leq NX - 1 \end{aligned}$$

In Equation 20, the convective term (second term, left side) is hyperbolic in nature. The single point upstream weighting causes artificial numerical dispersion. Numerical dispersion smears concentration fronts resulting in lower predictions of oil recovery<sup>20</sup>. For that reason, more accurate higher order methods have been proposed<sup>23</sup>.

## 2.5 Solution algorithm

When the solution at the  $k$ -iteration is known the solution at the  $k+1$ -iteration is calculated with the following algorithm.

- Step 1 - Calculating aqueous phase pressure from Equation 17.
- Step 2 - Calculating oleic phase pressure from Equation 3.
- Step 3 - Calculating Darcy's velocities from Equations 18, 19 and 6.
- Step 4 - Calculating overall chemical and petroleum concentrations from Equations 20
- Step 5 - Calculating overall water concentration, volume fractions and phase saturations by means of Equations 8 ( $i = p, c$ ), 9 ( $j = o, a$ ), 10, 11, 1, 2 and 3.
- Step 6 - Evaluating errors: two norms are calculated,

$$\sum_{m=1}^{NX} \left| (Z_i)_m^{n+1,k+1} - (Z_i)_m^{n+1,k} \right| ; \quad i = p, c \quad (21)$$

When the sum of both norms is lower than a pre-established error,  $\varepsilon$ , the  $k+1$ -iteration is finished and calculations start again for a new level of time. Otherwise, a new iteration is started from Step 1.

### 3 PHYSICAL PROPERTY DATA

#### 3.1 Partition of the components between the phases: the phase behavior model

The three pseudo-component system is represented on a ternary diagram (Figure 1) where the chemical component is located on top, the water on bottom left and the petroleum on bottom right. The composition of the mixture is represented by a point inside the triangle (Figure 1.3). That point is completely determined by any of two overall concentrations  $Z_i$  ( $i=p, w, c$ ), because the third is found by Equation 11.

As the concentration of the chemical component increases, petroleum and water become miscible. Therefore, a binodal curve divides the triangle in two zones: the miscible zone on top and the immiscible two-phase zone on bottom. So as to describe the phase diagram by a mathematical model, a binodal curve made up of two straight lines has been proposed<sup>10,19</sup> (Figure 1.1 – 1.10).

In the immiscible zone, tie-lines (dashed lines) indicate the coexistence of two phases (see, for example, Figure 1.8): (1) an aqueous solution with a volume fraction of water  $V_w^a$ , which has solubilized a volume fraction of chemical  $V_c^a$  and a volume fraction of petroleum  $V_p^a$ ; and (2) an oil phase with a volume fraction of petroleum  $V_p^o$ , which has been swelled by a volume fraction of chemical  $V_c^o$  and a volume fraction of water  $V_w^o$ . The miscibilization of oil into the aqueous phase is called “solubilization”, and the miscibilization of chemical and water into the oil phase is called “swelling”<sup>10,11,19</sup>. In the immiscible zone, as the chemical concentration increases, tie-lines get increasingly shorter. They disappear at the plait point, on the binodal curve.

The interior triangle is described by the solubilization parameter,  $L_{pc}^a$  and the swelling parameter,  $L_{wc}^o$ , defined as,

$$L_{pc}^a = \frac{V_p^a}{V_c^a} \quad (22)$$

$$L_{wc}^o = \frac{V_w^o}{V_c^o} \quad (23)$$

Equations 21 and 23 represent the magnitude of solubilization of the petroleum component into the aqueous phase and the magnitude of swelling of the oleic phase by water.

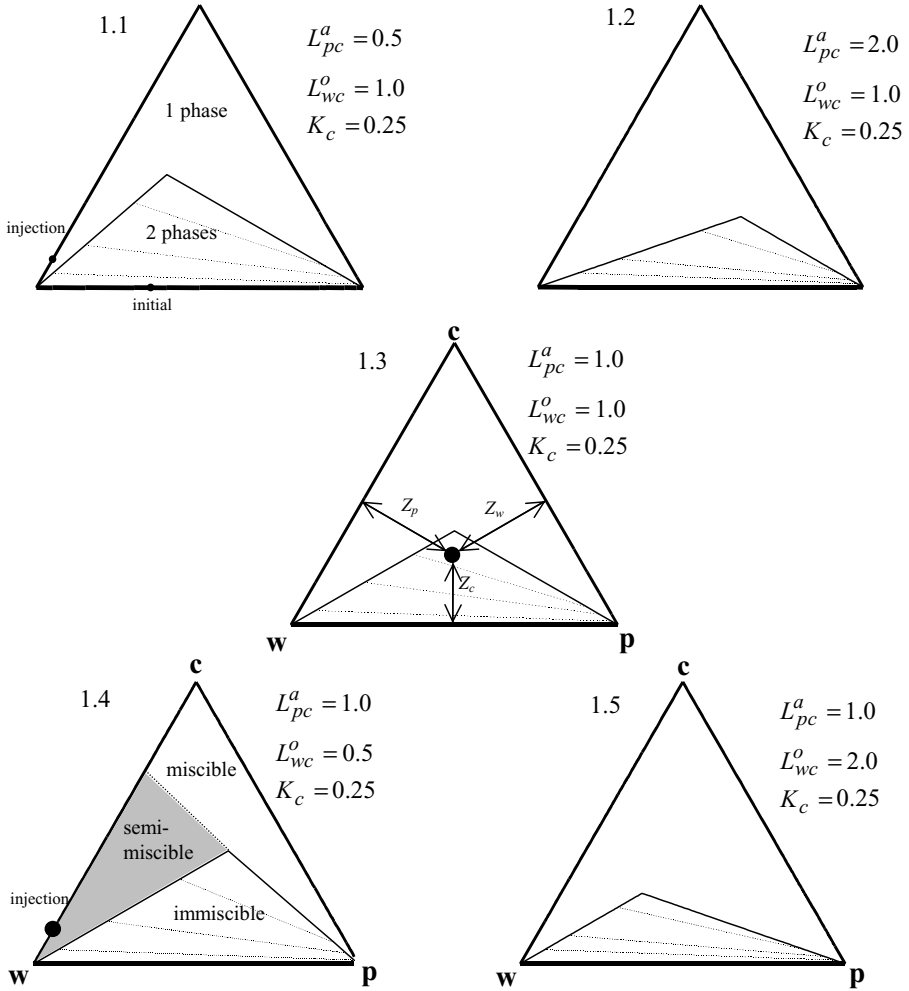


Figura 1.1-1.5. Ternary diagrams of type II(-) phase behaviors.

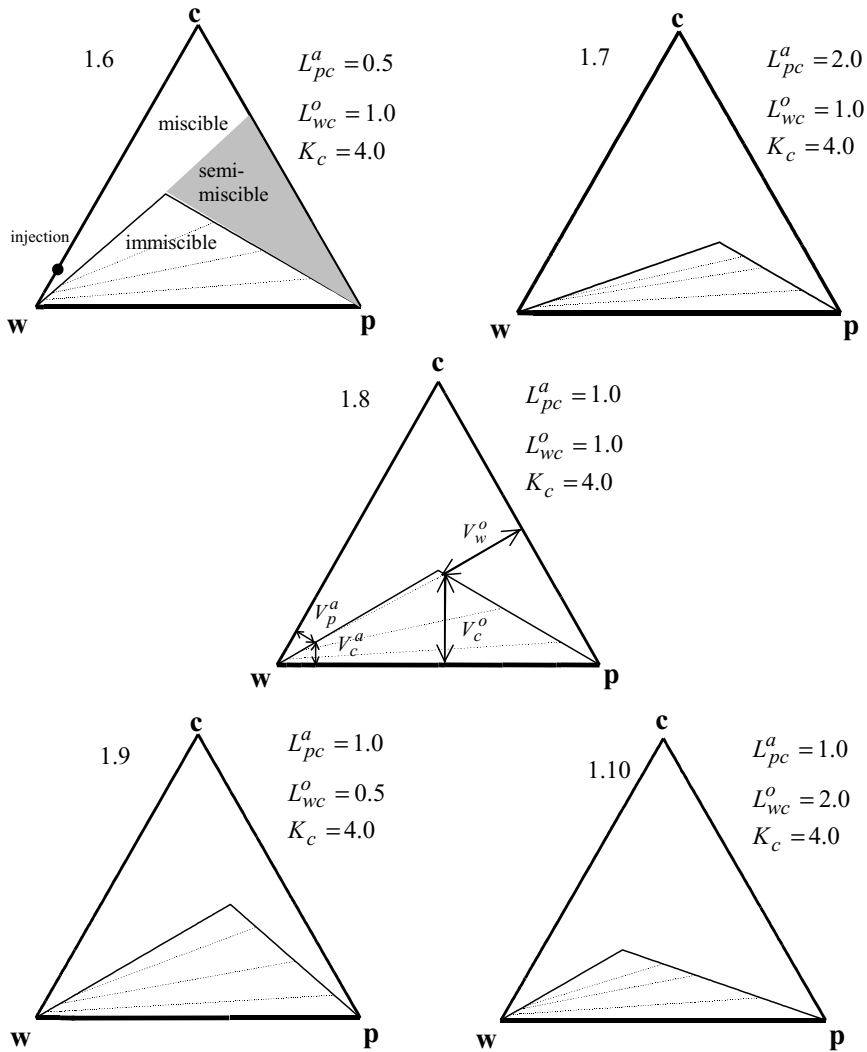


Figura 1.6-1.10. Ternary diagrams of type II(+) phase behaviors.

The slopes of the tie-lines are determined by the partition coefficient,  $K_c$ , which is the ratio of the chemical concentration in the oleic phase to that in the aqueous phase,

$$K_c = \frac{V_c^o}{V_c^a} \quad (24)$$

Therefore, the phase diagram is characterized only by three constant parameters:  $L_{pc}^a$ ,  $L_{wc}^o$  and  $K_c$ . This is a simple way to represent phase behavior. But it describes systems with most of the chemical in the aqueous phase, Type II(-), and with most of the chemical in the oleic phase, Type II(+). Figures 1.1-1.5 represent Type II(-) with negative slopes of the tie-lines, and so  $K_c < 1$ . Conversely, Figures 1.6-1.10 represent Type II(+) systems with positive slopes of the tie-lines, and so  $K_c > 1$ .  $K_c$  values can be modified by changing, for instance, the composition of the injected chemical, the temperature and/or the water salinity.

In order to analyze the influence of three coefficients defined by Equations 22, 23 and 24 upon the results, the following values have been chosen.

$$L_{pc}^a = 0.5, 1.0, 2.0 \quad ; \quad L_{wc}^o = 0.5, 1.0, 2.0 \quad ; \quad K_c = 0.25, 4.0 \quad (25)$$

These values have been combined as shown in Figures 1.1-1.10.

### 3.2 Interfacial tension

Interfacial tension for Type II(-) phase behavior systems (plait point on the right) is described by<sup>9,19</sup>,

$$\begin{aligned} \log \sigma &= \log F + \left(1 - L_{pc}^a\right) \log \sigma^H + \frac{G_1}{1 + G_2} L_{pc}^a \quad ; \quad L_{pc}^a \leq 1 \\ \log \sigma &= \log F + \frac{G_1}{(1 + L_{pc}^a G_2)} \quad ; \quad L_{pc}^a > 1 \end{aligned} \quad (26)$$

Similarly, for Type II(+) phase behavior systems (plait point on the left) interfacial tension is expressed as,

$$\begin{aligned} \log \sigma &= \log F + \left(1 - L_{wc}^o\right) \log \sigma^H + \frac{G_1}{1 + G_2} L_{wc}^o \quad ; \quad L_{wc}^o \leq 1 \\ \log \sigma &= \log F + \frac{G_1}{(1 + L_{wc}^o G_2)} \quad ; \quad L_{wc}^o > 1 \end{aligned} \quad (27)$$

$\sigma^H$  is the interfacial tension in a water-oil (no chemical) system,  $G_1$  and  $G_2$  are constant parameters and  $F$  is a factor which reduces the interfacial tension to zero as the composition approaches the plait point.  $F$  is obtained from,

$$F = \frac{1 - e^{-\sqrt{\sum_{i=p,w,c} (V_i^o - V_i^a)^2}}}{1 - e^{-\sqrt{2}}} \quad (28)$$

Equations 26 and 27 define a two-parameter IFT model<sup>19</sup> which is a simplification of a experimentally verified six-parameter model<sup>8,9,13</sup>.

Typical values for  $G_1$  and  $G_2$  parameters have been chosen<sup>19</sup>.

$$G_1 = -1.7 \quad ; \quad G_2 = -0.02 \quad (29)$$

In our example, oil trapped after waterflooding is displaced by the injection of an slug of surfactant solution. The surfactant solution lowers the oil-water interfacial tension and, thus mobilizes the trapped oil. Therefore, residual oleic phase saturation for the water-oil-surfactant system depends on interfacial tension.

### 3.3 Residual saturation

Residual phase saturations,  $S^{jr}$ , are functions of  $\sigma$ , the interfacial tension between the fluid phases. This functionality is described through the dimensionless capillary number,  $N_{VC}$ , which is the ratio of viscous to capillary forces.  $N_{VC}$  is defined by,

$$N_{VC} = \frac{uK}{\lambda\sigma} \quad (30)$$

$u$  is the total Darcy velocity (Equation 2),  $\lambda$  is the total mobility (Equation 4). The relationship between residual phase saturations and the capillary number has been called *capillary desaturation curve*<sup>13</sup>:

$$\frac{S^{jr}}{S^{jrH}} = \begin{cases} 1 & \text{if } N_{vc} < 10^{(1/T_1^j) - T_2^j} \\ T_1^j \left[ \log(N_{vc}) + T_2^j \right] & \text{if } 10^{(1/T_1^j) - T_2^j} \leq N_{vc} \leq 10^{-T_2^j} \quad j = o, a \\ 0 & \text{if } N_{vc} > 10^{-T_2^j} \end{cases} \quad (31)$$

where  $\frac{S^{jr}}{S^{jrH}}$  is a normalized  $j$ -phase residual saturation (superscript  $H$  represents the water-oil high interfacial tension system), and  $T_1^j$  and  $T_2^j$  are the trapping parameters (constants).

Normalized residual saturation as a function of capillary number for both aqueous and oleic phases are plotted in Figure 2 considering the following trapping parameter values,

$$T_1^j = -0.6; \quad j = o, a \tag{34}$$

$$T_2^o = 1.57; \quad T_2^a = -0.7 \tag{35}$$

Parameters in Equations 34 and 35 correspond to a water-wet reservoir. The wetting-phase requires considerably lower interfacial tension values to achieve its complete desaturation ( $S^{ar} = 0$ ), compared to those values in which the non-wetting phase is thoroughly desaturated ( $S^{or} = 0$ ).

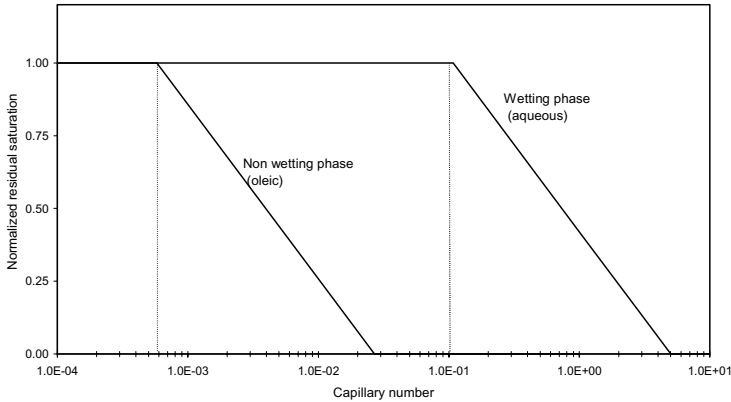


Figure 2. Capillary desaturation curves for wetting and non wetting phases. Normalized residual saturation  $S^{jr}/S^{j^rH}$  as a function of capillary number  $N_{VC}$

### 3.4 Relative permeabilities

Relative permeabilities are calculated from Camilleri *et al*<sup>12</sup>

$$k_r^j = k_r^{j0} \left( \frac{S^j - S^{j^r}}{1 - S^{j^r} - S^{j^r}} \right)^{e^j}; \quad j = o, a; \quad j^i = a, o; \quad j \neq j^i \tag{36}$$

where  $k_r^{j0}$  and  $e^j$  represent the endpoint and curvature of the function  $k_r^j(S^j)$ . This function is called the relative permeability curve of phase  $j$ . The  $j$ -phase residual saturation,  $S^{jr}$ , is obtained from the capillary desaturation curves represented by Equations 31, 32 and 33. The  $j$ -phase relative permeability endpoint and curvature are considered as functions of the  $j^i$ -phase residual saturation as follows,

$$k_r^{j0} = \left(1 - k_r^{j0H} \left(1 - \frac{S^{j'r}}{S^{j'rH}}\right)\right) + k_r^{j0H} ; j = o, a ; \quad j' = a, o ; \quad j \neq j' \quad (37)$$

$$e^j = \left(1 - e^{jH} \left(1 - \frac{S^{j'r}}{S^{j'rH}}\right)\right) + e^{jH} ; j = o, a ; \quad j' = a, o ; \quad j \neq j' \quad (38)$$

$k_r^{j0H}$ , and  $e^{jH}$  are the end point and the exponent for the water-oil (no chemical) high interfacial tension system. Equations 36-38 qualitatively describe laboratory measurements<sup>19</sup>.

### 3.5 Phase viscosities

The viscosity of any phase  $j$  is a function of composition,

$$\mu^j = V_w^j \mu^{aH} e^{\alpha_1(V_p^j + V_c^j)} + V_p^j \mu^{oH} e^{\alpha_1(V_w^j + V_c^j)} + V_c^j \alpha_3 e^{\alpha_2(V_w^j + V_p^j)} ; \quad j = o, a \quad (39)$$

All  $\alpha$  parameters are constant;  $\mu^{aH}$  and  $\mu^{oH}$  are the viscosities of the aqueous and oleic phases in the water-oil (high IFT) system. Camilleri *et al*<sup>12</sup> compared viscosities estimated in Equation 39 with experimental data. They agree reasonably well.

### 3.6 Other data

$\Delta x_D = 0.01$	$Z_c^{IN} = 0.1$	$e^{aH} = 1.5$
$\Delta t_D = 0.0005 \text{PV}$	$Z_p^{IN} = 0$	$G_1 = -1.7$
$\varepsilon = 0.005$	$t_{Ds} = 0.2 \text{PV}$	$G_2 = -0.02$
$NX = 101$	$L = 100 \text{ cm}$	$\mu^{aH} = 1 \text{ cp}$
$u^{IN} = 10^{-4} \text{ cm/s}$	$\sigma^H = 20 \text{ din/cm}$	$\mu^{oH} = 5 \text{ cp}$
$S^{orH} = S^{arH} = 0.35$	$k_r^{o0H} = 1$	$\alpha_1 = \alpha_2 = 0$
$P_i = P_e = 1 \text{ atm}$	$k_r^{a0H} = 0.2$	$\alpha_3 = 1$
$\phi = 0.24$	$e^{oH} = 1.5$	$K = 0.5 \text{ D}$

Table 1- Reservoir properties and simulation parameters

A set of common data is given in Table I. It represents a dynamic test performed on a reservoir rock sample. A constant composition ( $Z_c^{IN} = 0.1$ ) chemical slug is injected during 0.2 PV, followed by a continuous bank of water. Dimensionless distance,  $x_D$  and dimensionless time,  $t_D$  (number of injected pore volumes) are defined by,

$$x_D = \frac{x}{L}; \quad t_D = \frac{u^{IN} t}{\phi L} = PV^{IN} \quad (40)$$

where  $L$  is the total length and  $u^{IN}$  is the Darcy's velocity at inlet.

In the following results, capillary pressure, adsorption and dispersion have been neglected.

### 3.7 Physical property measurements and relationships

Physical property data of Table 1 have been taken from the literature<sup>7-14,19</sup>. They are typical of specific oil-water-surfactant systems. For an actual oil-water-chemical system, many measurements should be performed. They can be divided as statical and dynamical measurements.

Statical properties are phase behavior, interfacial tension, phase viscosities, wettabilities, etc.

Dynamical properties are residual saturations and relative permeabilities. They are determined by laboratory tests performed on linear corefloods using the actual oil-water-chemical system. Pressures, flow rates and component concentrations are measured at the core inlet and outlet. These dynamical tests allow the determination of residual saturations and relative permeabilities by an inverse method.

The relationship among physical properties is represented in Figure 3.

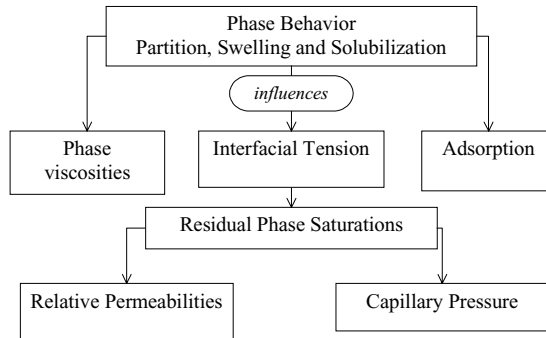


Figure 3. Physical properties relationships of data.

## 4 RESULTS

A sensitivity analysis of the influence of phase behavior on the oil recovery (percent of residual oil left after waterflooding) is presented in Figures 4.1-4.4. Phase behavior data are the ten ternary diagrams of Figures 1.1-1.10. Reservoir properties and simulation parameters are shown in Table I.

The three curves of cumulative oil recovered vs injected pore volumes of Figure 4.1

correspond to ternary diagrams of Figures 1.1, 1.3 and 1.2. Oil recovery is lower for the phase behavior of Figure 1.1. This is so for two reasons. First, the immiscible zone (interior triangle) is bigger than those of Figures 1.3 and 1.2. Second, the distance between the injection point and the binodal interior triangle along the extended tie-line which passes through the injection is shorter for Figure 1.1 than for the other two figures. That distance depends on the solubilization parameter,  $L_{pc}^a$ . Oil recovery is higher for phase behavior of Figure 1.2 because the opposite reasons. And intermediate for the oil recovery curve corresponding to ternary diagram of Figure 1.3.

The three curves of cumulative oil recovered vs injected pore volumes of Figure 4.2 correspond to ternary diagrams of Figures 1.4, 1.3 and 1.5. The sequence of the three oil recovery curves is qualitatively similar to that of Figure 4.1. However the differences in oil recovery values is much smaller. This is because only the first reason above mentioned is kept in this case. The distance between the injection point and the binodal interior triangle along the extended tie-line which passes through the injection is exactly the same for Figures 1.4, 1.3 and 1.5, which have the same solubilization parameter.

In the ternary diagram three regions can be distinguished<sup>10</sup>: immiscible, miscible and semi-miscible. Immiscible is the two-phase zone delimited by the interior triangle. The single-phase region can be divided in miscible and semi-miscible regions by the extended tie line which forms the side of the interior triangle. This is illustrated in Figure 1.4 and 1.6. The slug composition is a solution of 10 percent chemical (surfactant) in water. Therefore the injected composition lies in the semi-miscible region for type II(-) systems of Figures 1.1-1.5, and in the miscible region for type II(+) systems of Figures 1.6-1.10. After injection, slugs of the latter systems “travel” miscibly along the core. A miscible displacement should recover more oil.

In effect, cumulative oil recovered is higher in Figures 4.3 and 4.4 corresponding to type II(+) systems. In Figure 4.3, for a solubilization parameter of 2.0 recovery attains 100 per cent. Recovery decreases as solubilization parameter does. The same can be said of Figure 4.4. Let us notice that there for a swelling parameter  $L_{wc}^o = 0.5$  the recovery is the much lower than for swelling parameters of 1.0 and 2.0. In the former case when the slug enters the immiscible zone, the interfacial tension is higher than in the latter cases (compare Equation 27 with swelling parameters= 0.5, 1.0 and 2.0). Consequently, the capillary number decreases and through the capillary desaturation curve (Figure 2) the residual oleic saturation increases. Therefore, the relative permeability of the oleic phase gets more unfavorable. This case best illustrates the coupling of the recovery mechanisms. A similar explanation is valid for Figure 4.1 for a solubilization parameter of 0.5, examining Equation 26 which rules the interfacial tension.

## 5 CONCLUSIONS

1. Numerical simulation of a three-component, two-phase surfactant flooding is presented. It describes a one-dimensional laboratory displacement, where an slug of aqueous surfactant solution is injected, followed continuously by water .
2. The phase behavior of the three components, that partition between the two phases, is represented on a ternary diagram. The two phase immiscible region is delimited by the sides of a small interior triangle (binodal envelope). And it is defined by three parameters: the partition, solubilization and swelling coefficients.
3. Miscible, semi-miscible and immiscible displacements are distinguished on the ternary diagram by the position of the injected composition relative to that small triangle extended tie line.
4. The simulator considers physical properties– such as interfacial tension, residual saturations, relative permeabilities, phase viscosities, etc, that are dependent functions of concentration and, hence, of phase behavior. Measurement of these properties is difficult, among other problems, because of their intricate and complex relationships.
5. A sensitivity analysis of the influence of the partition, solubilization and swelling coefficients on cumulative oil recovered as a function of time shows that: a) Higher partition coefficients achieved better oil recoveries. b) For a fixed partition coefficient value, higher solubilization and swelling coefficients attain better oil recoveries.
6. Phase behavior modifies interfacial tension, residual saturations and relative permeabilities. In turn , every property affect oil recovery. For our data, the coupling effects of those properties is best illustrated in two cases that give very small oil recoveries: a) Partition and solubilization coefficients less and than one. b) Partition coefficient more than one and swelling coefficient less and than one. In both cases, solubilization and swelling coefficients less than one cause high interfacial tension immiscible displacement.

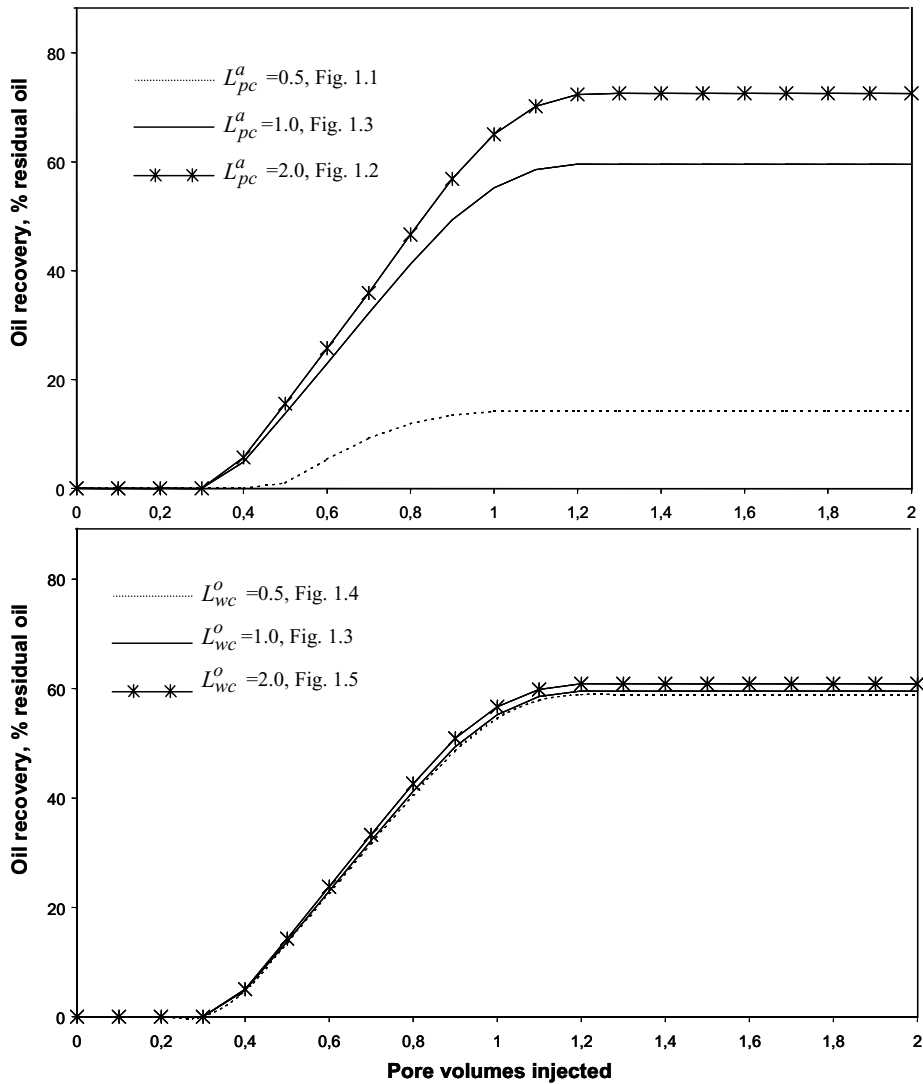


Figure 4 – Oil recovery as a function of pore volumes injected for Type II(-) systems,  $K_c = 0.25$ .

4.1 above: sensitivity to  $L_{pc}^a$ , with  $L_{wc}^o = 1$ . 4.2 below: sensitivity to  $L_{wc}^o$ , with  $L_{pc}^a = 1$

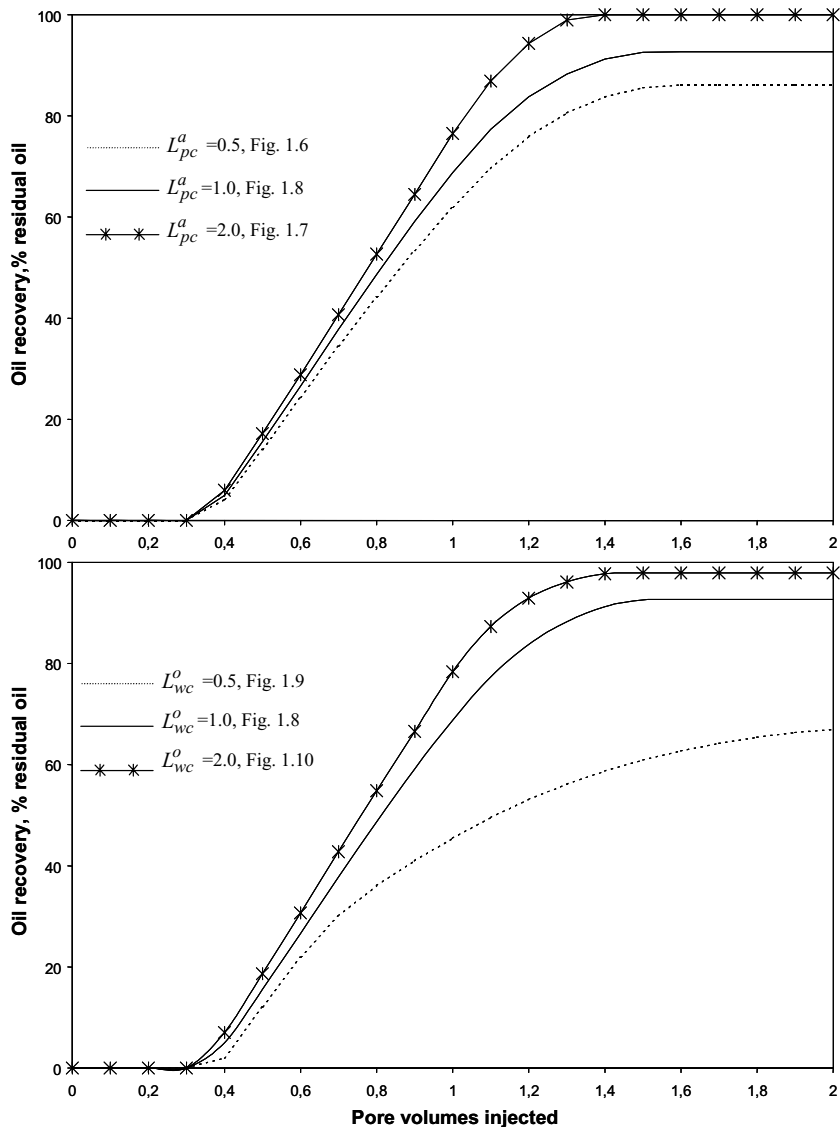


Figure 4 cont. – Oil recovery as a function of pore volumes injected for Type II(+) systems,  $K_c = 4.0$ .

4.3 above: sensitivity to  $L_{pc}^a$ , with  $L_{wc}^o = 1$ . 4.4 below: sensitivity to  $L_{wc}^o$ , with  $L_{pc}^a = 1$ .

## 6 NOMENCLATURE

$A$	= cross-sectional area of reservoir (cm <sup>2</sup> ).
$Ad$	= adsorbed volume of component per unit volume of the porous medium.
$D$	= dispersion coefficient (cm <sup>2</sup> /s)
$e$	= relative permeability exponent.
$F$	= interfacial tension factor defined in Equation 11.
$G_1, G_2$	= interfacial tension parameters, defined in Equations 10.
$K$	= absolute permeability (Darcy)
$K_C$	= chemical partition coefficient, defined in Equation 3.
$k_r$	= relative permeability.
$L$	= length of system (cm)
$L_{pc}^a$	= solubilization parameter, defined in Equation 1.
$L_{wc}^o$	= swelling parameter, defined in Equation 2
$N_{VC}$	= capillary number, defined in Equation 4.
$NX$	= total number of grid blocks.
$P$	= pressure (atm)
$P_C$	= capillary pressure (atm)
$P_e$	= pressure at the outlet boundary (atm)
$P_i$	= initial pressure (atm)
$S$	= saturation
$S^{ar}$	= aqueous phase residual saturation
$S^{or}$	= oleic phase residual saturation.
$t$	= time (s)
$T_1^j, T_2^j$	= $j$ -phase trapping parameters, defined in Equations 5, 6 and 7.
$u$	= Darcy's velocity (cm/s)
$V$	= volume fraction
$x$	= distance along porous sample (cm)
$Z$	= overall concentration

### Greek Letters

$\alpha_1, \alpha_2, \alpha_3$	= phase viscosity parameters defined in Equation 14.
$\lambda$	= phase mobility, defined in Equations 4 and 5
$\sigma$	= interfacial tension (din/cm)
$\sigma_{min}^j$	= minimum interfacial tension value, below which the $j$ -phase is thoroughly desaturated din/cm)
$\phi$	= porosity
$\mu$	= viscosity (cp)
$\epsilon$	= iteration error

### Subscripts

$i$	= component.
$c$	= chemical component.
$D$	= dimensionless.
$m$	= grid block number.
$p$	= petroleum component.
$w$	= water component.
$s$	= slug

### Superscripts

$0$	= endpoint of function
$a$	= aqueous phase
$H$	= water-oil (no chemical) high interfacial tension system.
$IN$	= injection
$j$	= phase
$k$	= iteration level
$n$	= time-step number
$o$	= oleic phase
$r$	= residual

## 7 ACKNOWLEDGEMENTS

This research was supported by the Agencia Nacional de Promoción Científica y Tecnológica, PECOM Oil Co., the University of Buenos Aires and the University of Cuyo. M. S. Bidner and G. B. Savioli are members of the Career of Scientific Research at the Consejo Nacional de Investigaciones Científicas y Técnicas (all in Argentina).

**8 REFERENCES**

- [1] M. S. Bidner, Propiedades de la Roca y los Fluidos de los Reservorios de Petróleo. EUDEBA, (2001).
- [2] W. L. Lake, *Enhanced Oil Recovery*, Prentice-Hall (1989).
- [3] L.W. Lake, G.A. Pope, G.F. Carey, and K. Sepehrnoori, "Isothermal, Multiphase, Multicomponent Fluid Flow in Permeable Media - Part I : Description and Mathematical Formulation", *In Situ*, **8** No.1, 1-40, (1984).
- [4] F. G. Helfferich, "Theory of Multicomponent, Multiphase Displacement in Porous Media," *Soc. Pet. Eng. J.*, **21** No.1, 51-62 (1981)
- [5] P.D. Fleming, C. P. Thomas, W.K. Winter, "Formulation of a General Multiphase Multicomponent Chemical Flood Model," *Soc. Pet. Eng. J.*, **21** No.1, 63-76, (1981)
- [6] L.W. Lake, G.A. Pope, G.F. Carey, and K. Sepehrnoori, "Isothermal, Multiphase, Multicomponent Fluid Flow in Permeable Media, Part II: Numerical Techniques and Solutions," *In Situ*, **8** No.1, 41-97, (1984).
- [7] R. G. Larson and G.J. Hirasaki, "Analysis of the Physical Mechanisms in Surfactant Flooding," *Soc. Pet. Eng. J.* **18**, No.1, 42-58 (1978).
- [8] G.A. Pope, B. Wang and K. Tsaur, "A Sensitivity Study of Micellar/Polymer Flooding," *Soc. Pet. Eng. J.*, **19** No.6, 357-368 (1979)
- [9] G. J. Hirasaki, "Application of the Theory of Multicomponent, Multiphase Displacement to Three-Component, Two-Phase Surfactant Flooding," *Soc. Pet. Eng. J.*, **21** No.2, 191-204 (1981)
- [10] R. G. Larson, "The Influence of Phase Behavior on Surfactant Flooding," *Soc. Pet. Eng. J.*, **19** No.6, 411-422 (1979).
- [11] R. G. Larson, H. T. Davis and L. E. Scriven, "Elementary Mechanisms of Oil Recovery by Chemical Methods," *Journal of Pet. Tech.*, **34**, 243-258 (1982).
- [12] D. Camilleri, S. Engelsen, L.W. Lake, E.C. Lin, T. Ohno., G.A. Pope and K. Sepehrnoori, "Description of an Improved Compositional Micellar/Polymer Simulator," *Soc. Pet. Eng. Res. Eng.*, **2** No.4, 427-432. (1987).
- [13] D. Camilleri, A. Fil., G.A. Pope, B.A. Rouse and K. Sepehrnoori, "Improvements in Physical-Property Models Used in Micellar/Polymer Flooding," *Soc. Pet. Eng. Res. Eng.* **2** No.4, 433-440 (1987).
- [14] D. Camilleri, A. Fil., G.A. Pope, B.A. Rouse and K. Sepehrnoori, "Comparison of an Improved Compositional Micellar/Polymer Simulator With Laboratory Corefloods," *Soc. Pet. Eng. Res. Eng.*, **2** No.4, 441-451 (1987).
- [15] M. Delshad, K. Asakawa, G.A. Pope and K. Sepehrnoori., "Simulations of Chemical and Microbial Enhanced Oil Recovery Methods," Society of Petroleum Engineers Paper #75237, *Proceedings of the SPE Thirteenth Symposium on Improved Oil Recovery*, Tulsa, OK, (2002).
- [16] N. Saad, G. A. Pope and K. Sepehrnoori, "Simulation of Big Muddy Surfactant Pilot," *Soc. Pet. Eng. Res. Eng.*, **4** No.1, 24-34 (1989).
- [17] P.C. Porcelli and M.S. Bidner, "Modelización de la Inundación, Química de Yacimientos Petrolíferos," *Revista Internacional de Métodos Numéricos para Cálculo y Diseño en Ingeniería*, **8** No. 2, 157-175 (1992).
- [18] P.C. Porcelli and M.S. Bidner, "Simulation and Transport Phenomena of a Ternary Two-Phase Flow," *Transport in Porous Media*, **14**, No. 2, 1-20 (1994).
- [19] M. S. Bidner and P. C. Porcelli, "Influence of Phase Behavior on Chemical Flood Transport Phenomena," *Transport in Porous Media*, **24**, N° 3, 247-273 (1996).
- [20] M. S. Bidner and P. C. Porcelli, "Influence of Capillary Pressure, Adsorption and Dispersion on Chemical Flood Transport Phenomena," *Transport in Porous Media*, **24**, N° 3, 275-296 (1996).
- [21] J. Bear, *Dynamics of Fluids in Porous Media*, American Elsevier, New York (1972).
- [22] K. A. Aziz and A. Settari, *Petroleum Reservoir Simulation*, Elsevier, New York (1979)
- [23] N. Saad, G. A. Pope and K. Sepehrnoori, "Application of Higher-Order Methods in Compositional Simulation," *Soc. Pet. Eng. Res. Eng.*, **5** No.4, 623-630 (1990).